Solar Cell Sensitizer Models [Ru(bpy-R)2(NCS)2] Probed by Spectroelectrochemistry

Sara Kämper,[†] Alexa Paretzki,[†] Jan Fiedler,[‡] Stanislav Záliš,[‡] and Wolfgang Kaim*,[†]

[†]Institut für Anorganische Chemie, Universität Stuttgart, Pfaffenwaldring 55, D-70550 Stuttgart, Germany
[‡]J. Heyrovský Institute of Physical Chemistry, v.v.i., Academy of Sciences of the Czech Republic, Dolejškova 3, CZ-18223 Prague, Czech Republic

S *Supporting Information*

ABSTRACT: Complexes [Ru(bpy-R)2(NCS)2], where R = H (**1**), 4,4'-(CO2Et)2 (**2**), 4,4'-(OMe)2 (**3**), and 4,4'-Me2 (**4**), were studied by spectroelectrochemistry in the UV−vis and IR regions and by in situ electron paramagnetic resonance (EPR). The experimental information obtained for the frontier orbitals as supported and ascertained by density functional theory (DFT) calculations for **1** is relevant for the productive excited state. In addition to the parent **1**, the ester complex **2** was chosen for its relationship to the carboxylate species involved for binding to TiO2 in solar cells; the donor-substituted **3** and **4** allowed for better access to oxidized forms. Reflecting the metal-to-ligand (Ru → bpy) charge-transfer characteristics of the compounds, the electrochemical and EPR results for compounds **1**−**4** agree with previous notions of one metal-centered oxidation and several (bpy-R) ligand-centered reductions. The first one-electron reduction produces extensive IR absorption, including intraligand transitions and broad ligand-to-ligand intervalence charge-transfer transitions between the one-electron-reduced and unreduced bpy-R ligands. The electron addition to one remote bpy-R ligand does not significantly affect the N−C stretching frequency of the Ru^{II}NCS unit. Upon oxidation of Ru^{II} to Ru^{III}, however, the single N−C stretching band exhibits a splitting and a shift to lower energies. The DFT calculations serve to reproduce and understand these effects; they also suggest significant spin density on S for the oxidized form.
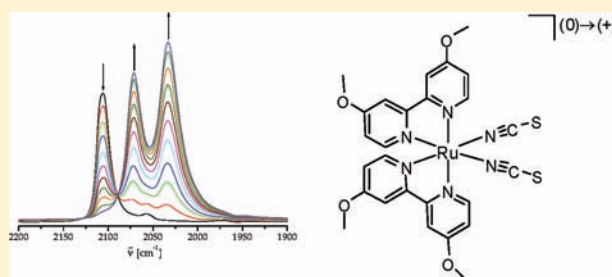
INTRODUCTION

In 1991, O'Regan and Grätzel described[1a] the design and function of a dye-sensitized solar cell (DSC), which has attracted widespread attention ever since.[1−6] One of the essential features of this original device has been association of the TiO2 particles and of an electrolyte solution with the sensitizing metal complex absorber. The main type of sensitizers employed has involved ruthenium polypyridine complexes with thiocyanato substituents, especially N3 and N719 (Scheme 1).[1−3]

Scheme 1

N3: X = H; N719: X = Bu4N
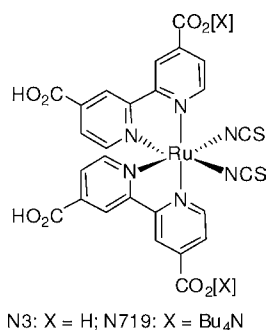
The [Ru(bpy-R)2(NCS)2] dyes at the center of DSCs serve to inject electrons into the semiconductor after metal-to-ligand charge-transfer (MLCT) excitation in a large part of the visible region.[1d] In addition, the high efficiency of DSCs involving thiocyanato substituents was attributed to the ultrafast (fs) electron injection and to a good contact with electrolyte components such as the I$^−$/I3$^−$ couple, possibly via the SCN$^−$ ligands;[4a,d,e] however, the lability of the nonchelating SCN$^−$ pseudohalide ligands has been recognized as an essential factor in eventually limiting the lifetime of such DSC devices.[4] The empirically established suitability of thiocyanatoruthenium compounds over other molecules still requires some rationalization. While numerous structural,[5] spectroscopic,[5] electrochemical,[4c,5a] and computational[6] studies have been performed for [Ru(bpy-R)2(NCS)2] complexes, of which only a representative selection can be cited here, we have now studied the model systems **1**−**4** (Figure 1) by spectroelectrochemistry. This method, whether applied in electron paramagnetic resonance (EPR) or in the IR and UV−vis−near-IR (NIR) spectral regions, combines energy (redox potentials) and mechanistic information from electrochemistry with the detailed characterization of electrogenerated intermediates or
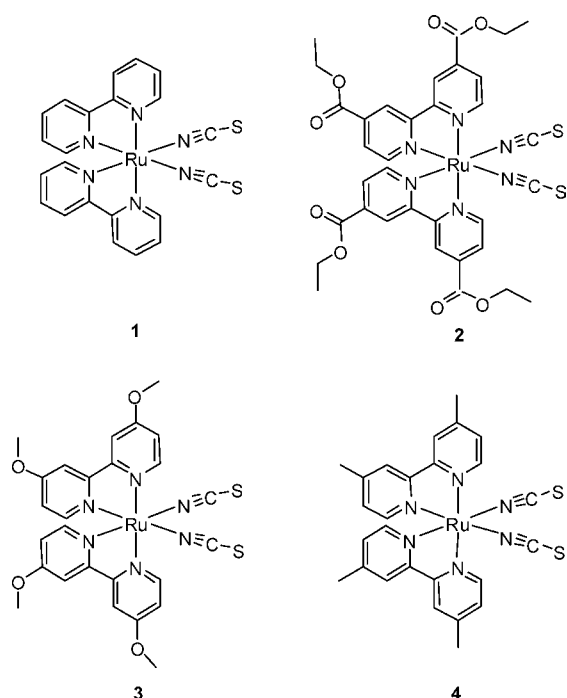
Figure 1. Complexes investigated (parent **1**, acceptor-substituted **2**, donor-substituted **3**, and **4**).

products by spectroscopic means.[7] Members of the "Ru-bpy" class of sensitizers have been studied in this way,[8] and thiocyanatoruthenium compounds related to **1**−**4** were also investigated by spectroelectrochemistry, e.g., on TiO₂ surfaces.[5e−i] However, these reports were limited to the UV−vis spectral range despite the presence of intense, well-separated N−C(S) vibrational stretching bands at around 2100 cm⁻¹.

It may be noted that the NCS ligand effects ligand-to-metal charge-transfer (LMCT) absorption and spin-crossover behavior[9] in its complexes with the lighter homologue, iron.

In addition to the parent **1**, we have chosen the ester complex **2** because of its relationship to the carboxylate species involved for TiO₂ binding in the DSC devices; the acceptor-substituted **2** is complemented by the donor-substituted **3** and **4** (Figure 1) in order to have experimentally easier access to oxidized as well as reduced forms. Density functional theory (DFT) calculations including solvent correction (polarizable continuum model, PCM) were used to analyze the experimental results and to discuss the possible ambient behavior[10] of the NCS ligand.

EXPERIMENTAL SECTION

Compounds **1** and **2** were prepared according to published procedures.[5,11] The donor-substituted compounds **3** and **4** were obtained in analogy by reacting KSCN in 10-fold excess with [Ru(bpy-R)₂Cl₂] in N,N-dimethylformamide (DMF) solution for 5 h under reflux. Removal of the solvent, extraction of excess KSCN with water, and washing with a little acetonitrile produced dark-red compounds, which were purified by column chromatography (silica) using dichloromethane (**3**) or 2:1 DMF/CH₃OH (**4**) as eluents. Typical yield: 90%. Data for **3**. ¹H NMR (DMF-d_7): 3.95 (s, 6 H, OCH_3), 4.15 (s, 6 H, OCH_3), 6.93 (dd, 2 H, 5′-H, ^4J = 2.7 Hz, ^3J = 6.6 Hz), 7.50−7.56 (m, 4 H, 5-H, 6′-H), 8.26−8.28 (m, 2 H, 3′-H), 8.38−8.41 (m, 2 H, 3-H), 9.15 (dd, 2 H, 6-H, ^4J = 2.7 Hz, ^3J = 6.6 Hz). Anal. Calcd for C₂₆H₂₄N₆O₄RuS₂: C, 48.06; H, 3.72; N, 12.94. Found: C, 48.13; H, 3.49, N, 12.86. HRMS (ESI). Calcd for C₂₆H₂₄N₆O₄RuS₂Na: m/z 673.0242. Found: m/z 673.0245. IR (solid): 2094, 2060sh, 1606, 1553,

1484, 1218, 1035, 1010, 831, 795 cm⁻¹. Data for **4**. ¹H NMR (DMSO-d_6): 2.39 (s, 6 H, CH_3), 2.65 (s, 6 H, CH_3), 7.07−7.09 (m, 2 H, 5′-H), 7.33−7.36 (m, 2 H, 6′-H), 7.74−7.76 (m, 2 H, 5-H), 8.45 (s, 2 H, 3′-H), 8.59 (s, 2 H, 3-H), 9.07−9.09 (m, 2 H, 6-H). Anal. Calcd for C₂₄H₂₄N₆RuS₂: C, 53.32; H, 4.13; N, 14.35. Found: C, 53.39; H, 4.17; N, 14.38. HRMS (ESI). Calcd for C₂₄H₂₄N₆RuS₂Na: m/z 609.0445. Found: m/z 609.0449. IR (solid): 2097, 1655, 1616, 1387, 823 cm⁻¹.

Instrumentation. EPR spectra in the X band (9.5 GHz) were recorded with a Bruker System EMX. UV−vis−NIR absorption spectra were recorded on J&M TIDAS and Shimadzu UV 3101 PC spectrophotometers. IR spectra were obtained using a Nicolet 6700 FTIR instrument. Cyclic voltammetry was carried out in 0.1 M Bu₄NPF₆ solutions using a three-electrode configuration (glassy carbon working electrode, platinum counter electrode, Ag/AgCl reference) and a PAR 273 potentiostat and function generator. The ferrocene/ferrocenium (Fc/Fc⁺) couple served as an internal reference. Spectroelectrochemistry was performed using an optically transparent thin-layer electrode (OTTLE) cell.[12] A two-electrode capillary served to generate intermediates for X-band EPR studies.[13]

Quantum Chemical Calculations. The electronic structures of complex [Ru(bpy)₂(NCS)₂]ⁿ, n = 0, 1+, 2+, 1−, 2−, were calculated by DFT methods using the *Gaussian 09*[14] and *ADF2010.01*[15,16] program packages.

For the H, C, N, O, and S atoms, 6-311G*-polarized triple-ζ basis sets[17] (G09) were used together with quasi-relativistic effective-core pseudopotentials and a corresponding optimized set of basis functions for Ru.[18] All structures were optimized without geometrical constraints using the hybrid PBE0 functional,[19,20] open-shell systems within the UKS approach. Vibrational analysis was done using structures optimized with the corresponding functional.

Slater-type orbital basis sets of triple-ζ quality with polarization functions for Ru and Re atoms and of double-ζ quality with polarization functions for the remaining atoms were employed within *ADF2010.01*. The inner shells were represented by the frozen-core approximation (1s for C, N, and O, 1s3d for Ru, and 1s4d for Re were kept frozen). The calculations were done with the functional including Becke's gradient correction[21] to the local exchange expression in conjunction with Perdew's gradient correction[22] to the local correlation (ADF/BP). The scalar relativistic zero-order regular approximation (ZORA) was used within ADF calculations. The **g** tensor was obtained from a spin-nonpolarized wave function after the incorporation of spin−orbit coupling. **A** and **g** tensors were obtained by first-order perturbation theory from a ZORA Hamiltonian in the presence of a time-independent magnetic field.[23]

PCM[24] was used for modeling of the solvent influence.

RESULTS AND DISCUSSION

Reflecting the MLCT (Ru → bpy) characteristics of this class of metal complexes,[25] the electrochemical results from cyclic voltammetry of compounds **1**−**4** agree with the notion[5a] of one metal-centered oxidation and several (bpy-R) ligand-centered reductions. Figures 2 and 3 show representative examples; however, as Table 1 indicates, not all processes are fully reversible under the conditions chosen. The data from Table 1 reflect the acceptor (**2**) and donor (**3** and **4**) substituent effects on the 2,2′-bipyridine ligand and suggest, for best results, to use **2** for spectroelectrochemical reduction and **3** for spectroelectrochemical oxidation. Reduction potentials at more negative values are likely to induce dissociation of the NCS⁻ pseudohalide ligands.

EPR studies confirm the notion of metal-centered oxidation[26] versus ligand-based reduction by showing a low-field-shifted signal for the most stable ruthenium(III) species **3**⁺ ($g_\parallel$ = 2.45; $g_\perp$ = 3.07) at 110 K in CH₂Cl₂/0.1 M Bu₄NPF₆ as opposed to essentially unresolved ruthenium(II)/radical-type spectra[13] with g_{iso} = 1.996 for **1**⁻ and g_{iso} = 1.995 for **2**⁻ (Figure S1 in the Supporting Information). DFT calculations based on
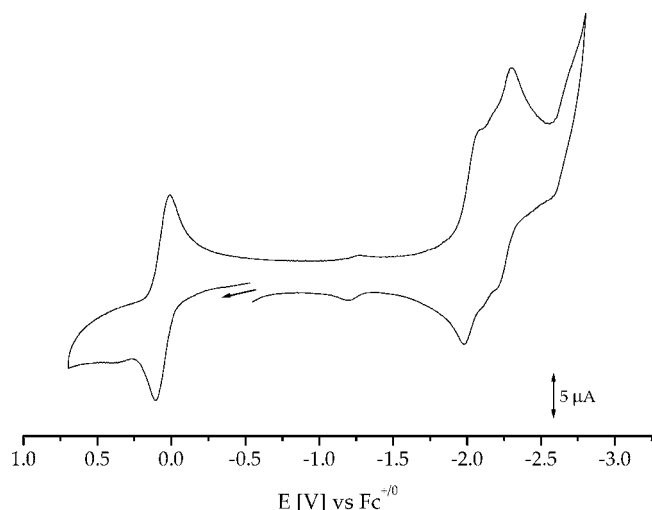
Figure 2. Cyclic voltammogram of **3** at 298 K in DMF/0.1 M Bu₄NPF₆ at 100 mV/s.
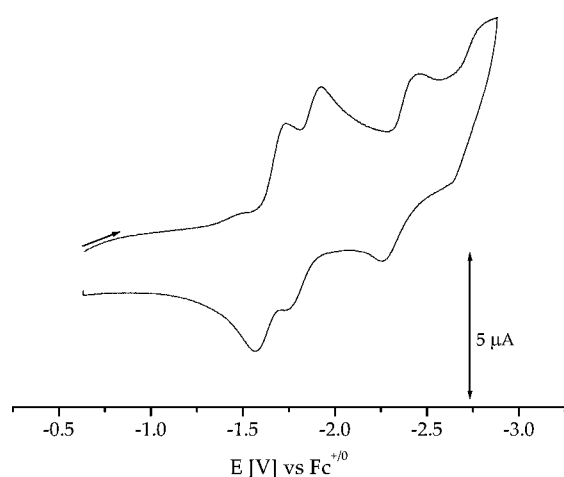
Figure 3. Cyclic voltammogram (reduction) of **2** at 215 K in DMF/0.1 M Bu₄NPF₆ at 100 mV/s.

Table 1. Half-Wave and Peak Potentials of 1−4 from Cyclic Voltammetry[a]

complex	$E_{1/2}(E_{pa}/E_{pc})$			
	1	2	3	4
oxidation	0.17 (0.21/0.12)	(0.48/−)	0.06 (0.01/0.11)	0.04 (0.11/−0.02)[b]
1. reduction	−2.00 (−1.96/−2.05)[b]	−1.65 (−1.57/−1.73)	(−/−2.11)	(−/−2.24)
2. reduction	(−/−2.20)	−1.87 (−1.94/−1.81)[b]	(−/−2.33)	(−/−2.48)

[a]In DMF/0.1 M Bu₄NPF₆ at a 100 mV/s scan rate; potentials in V vs Fc⁺/⁰. [b]Not fully reversible, i_p[backward]/i_p[forward] < 1.

geometry-optimized structures (Table 2) support these experimental results by showing bpy ligand-centered lowest unoccupied molecular orbitals (LUMOs) and metal-based highest occupied molecular orbitals (HOMOs) for the parent system **1** (Figure 4), in agreement with the results from earlier calculations of related compounds.[6] During oxidation, one electron is withdrawn from the metal-based HOMO, which contains an admixture of π NCS orbitals. DFT calculations with PCM correction confirm that the spin density in **1**⁺ (Figure 5)

Table 2. Selected G09/PBE0 Calculated Averaged Bond Lengths [Å] and Angles [deg] of [Ru(bpy)₂(NCS)₂]ⁿ

	$n = 0$		$n = +1$	$n = -1$
	calcd	exptl[a]	calcd	calcd
Bond Lengths (Å)				
Ru−N1(bpy)	2.051	2.041(4)	2.068	2.050
Ru−N2(bpy)	2.051	2.051(4)	2.087	2.040
Ru−N(NCS)	2.029	2.055(5)	1.969	2.045
N−C(NCS)	1.176	1.124(7)	1.184	1.172
C−S	1.620	1.654(7)	1.597	1.634
C2−C2′	1.466	1.452(8)	1.470	1.437
Angles (deg)				
N(NCS)−Ru−N(NCS)	93.3	88.7(3)	97.3	91.2
N(bpy1)−Ru−N(bpy1)	78.7	78.7(2)	78.2	79.2
N(bpy1)−Ru−N(bpy2)	177.8	173.0(5)	178.3	172.6
Ru−N−C(NCS)	169.8	168.2(5)	168.3	174.0
N−C−S	178.9	177.5(6)	178.5	178.8

[a]From ref 5d.
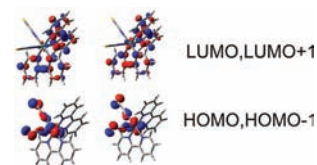
Figure 4. DFT-calculated (G09/PBE0/PCM) frontier orbitals of [Ru(bpy)₂(NCS)₂].
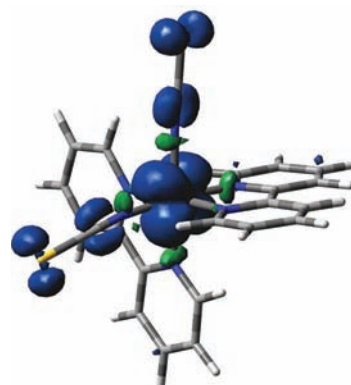
Figure 5. DFT-calculated (G09/PBE0/PCM) spin density of [Ru(bpy)₂(NCS)₂]⁺.

is largely metal-based (Ru, 0.746) with minor contributions from the thiocyanate ligands (N, 0.013; C, 0.001; S, 0.117) and on bpy (−0.009). The nonnegligible value of 0.117 on each S atom may have significance for the function of the photoexcited sensitizer, which is believed to interact with the electrolyte I⁻/I₃⁻ via the terminal S atoms of the NCS ligands.[4a,d,e] A thiocyanato-based HOMO, as suggested earlier[5h] for a related system, could not be confirmed here.

Significantly, the DFT calculations confirmed the experimentally established[5] N coordination of the ambidentate NCS ligand[10] for compounds like **1** (Table 2 and Figure S2 in the Supporting Information). The IR spectroelectrochemical results from the well-separated and usually intense N−C stretching bands of the thiocyanate ligands reflect that the [NCS]⁻ ion can be formulated via descriptions **A** and **B** with charges centered on S or N (Scheme 2). Note that **A** has triple-bond character for the C−N bond in contrast to the double

Scheme 2

bond for **B**, which can, however, participate in a cumulene situation S=C=N=M.

In addition to this electronic ambiguity, the terminal thiocyanato ligand is ambidentate ("schizophrenic") with N or S coordination to metals (linkage isomerism, bridging potential, etc.), including ruthenium examples (see Figure S2 in the Supporting Information).[10] Despite generalizing statements in textbooks implicating the hard/soft concept, the actual coordination is not always easy to predict.[10a,f] Compound **1**, for instance, clearly contains N-bonded NCS−; Table 4 (n = 0) shows that the N−C frequencies for the MSCN isomers are typically but not invariably[10a] shifted to higher wavenumbers in comparison with those of the MNCS isomer.

The molecular structures as found in the crystals of compounds such as **1−4** also reveal the expected cis configuration,[5] although only a single, hardly structured N−C stretching band is observed. This initially puzzling[5d] degeneracy of ν_{CN} has been explained by a "similarity in bonding properties of .... the two bpy ligands and the ... NCS− groups".[5d] In other words, the π back-donation from Ru[II] into the nitrile part of NCS− (structure **A**) produces an effect that is equivalent to the accepting function of the bpy ligands, thereby diminishing the splitting of symmetric and antisymmetric vibration combinations.

IR vibrational spectroelectrochemistry[7] in the ν_{NC} region around 2100 cm^{-1} was performed using an OTTLE cell;[12] ν_{CS} bands[5] (at lower energies) could not be studied because of interference from the strong absorption of the supporting electrolyte and solvent. Upon a one-electron reduction of electron-deficient **2**, the N−C stretching band shows virtually no effect, only a marginal decrease in the intensity and a 2 cm^{-1} shift to higher wavenumbers (Figure 6 and Table 3). The electron addition to remote and not directly connected bpy-R apparently does not affect the Ru[II]NCS unit. The second reduction of **2** produces a further minor shift of ν_{NC} and a band at 2056 cm^{-1}, assigned to dissociated [NCS]−, as expected from the multiple reduction of a pseudohalide complex.

Upon oxidation of Ru[II] to Ru[III], best studied for electron-rich **3**, the N−C stretching band exhibits a splitting and a considerable shift to lower energies, as shown in Figure 7 for **3**+ (Table 3).

While separation of the frequencies of symmetrical and antisymmetrical stretching combinations and the appearance of the two expected bands reflect the different behavior of anionic [NCS]− and neutral bpy toward the no longer π-donating Ru[III], the decreased capacity of Ru[III] for π back-donation seems to favor more contribution from structure **B** of [SCN]−, with a more negative charge on the metal-coordinated N atom and, hence, lower energy of N−C stretching. Correspondingly, the triple-bond character of the N−C bond from form **A** is partially reduced to a double bond in form **B**, reflected by the shift to smaller wavenumbers, which is qualitatively confirmed by DFT calculations (Tables 4 and 5). Table 5 presents the results of frequency calculations in solution models; these calculations correctly reproduce the NC frequency shift and splitting after oxidation.

Spectroscopic monitoring of the reduction of **2** in the NIR region showed the emergence of a broad absorption band

a)

b)
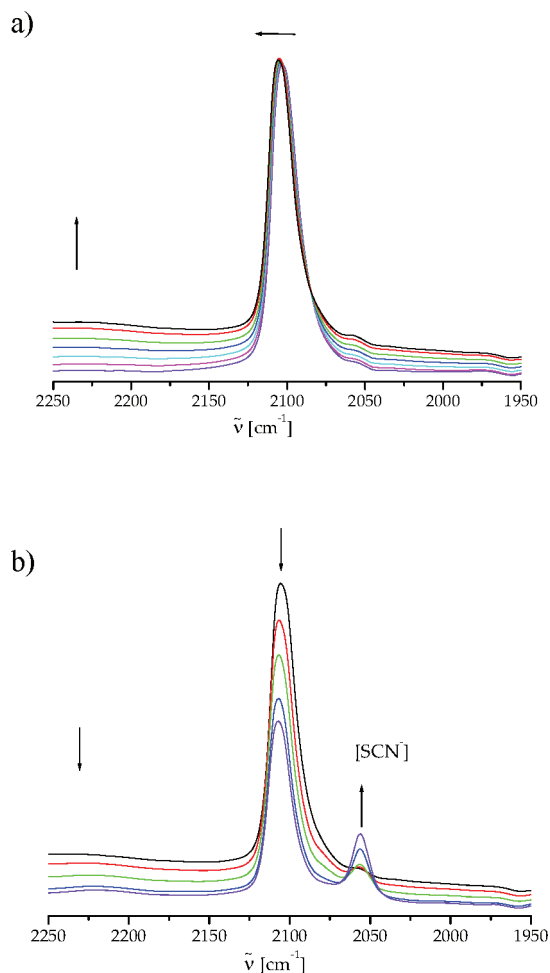
Figure 6. IR spectroelectrochemical response of **2** during first (a) and second reduction (b) in DMF/0.1 M Bu$_4$NPF$_6$.

Table 3. N−C(S) Stretching Vibrations (cm^{-1}) of Compounds 1−4 Following IR Spectroelectrochemistry^a

	$\tilde{\nu}_{NC}$			
	1	**2**	**3**	**4**
oxidation	2067, 2021		2071, 2033	2070, 2027
neutral state	2104	2103	2106	2105
1. reduction	2104	2105		
2. reduction		2107		

^{a}OTTLE spectroelectrochemistry at a platinum electrode in DMF/0.1 M Bu$_4$NPF$_6$.

system with shoulders and a maximum at about 1600 cm^{-1} (Figure 8a and Table 6), which can be attributed to an intraligand [IL; π*(7) → π*(8,9)] transition of the radical anion of the bpy derivative.[27] Such absorptions are well established and are distinguished by partially resolved vibrational structuring; their energy and intensity may vary significantly.[27,28] In accordance with this assignment, the reduction of the second bpy-R ligand to yield **2**$^{2-}$ causes an increase in the intensity of this band system (Figure 8b).

There is another, very broad electronic absorption feature emerging in the IR region upon going from **2** to **2**−, which, however, diminishes upon a second reduction (Figures 6 and 9). This absorption between about 1500 and 4500 cm^{-1} is only due to the ligand/ligand mixed-valent form **2**−; it disappears
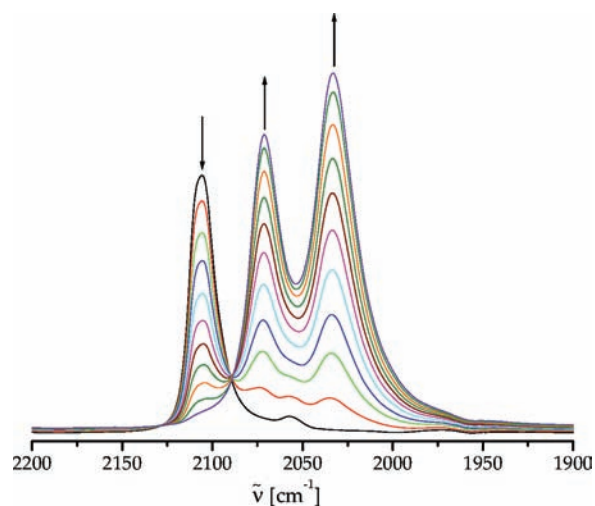
Figure 7. IR spectroelectrochemical response of **3** during oxidation in DMF/0.1 M Bu₄NPF₆.

Table 4. Experimental and in Vacuo DFT-Calculated (G09/PBE0) Stretching Frequencies ν_{NC} (cm⁻¹) of Different Isomers of $[Ru(bpy)_2(NCS)_2]^n$

	−NCS, −NCS		−SCN, −SCN	−NCS, −SCN
n	exptl	calcd[a]	calcd[a]	calcd[a]
0	2104	2100, 2109	2132, 2132	2102, 2131
1	2067, 2021	2041, 2051	2168, 2169	2036, 2168

[a]Scaled by a factor of 0.955.

Table 5. Experimental and in Solvento DFT-Calculated (G09/PBE0/PCM-DMF) Stretching Frequencies ν_{NC} (cm⁻¹) of $[Ru(bpy)_2(NCS)_2]^n$

	−NCS, −NCS	
n	exptl	calcd[a]
0	2104	2101, 2105
1	2067, 2021	2061, 2016

[a]Scaled by a factor of 0.945.

during the reduction to **2²⁻**. Consequently, it is attributed to a ligand-based intervalence charge transfer (LL′IVCT) between one-electron-reduced and unreduced bpy-R. Such weak LL′IVCT transitions can lie at very low energies, and the frequently broad bands[29] due to very large structural reorganization may thus go unnoticed. According to DFT calculations of **1**, LUMO and LUMO+1 are almost degenerate, suggesting an LL′IVCT transition at very low energies.

The MLCT absorptions of complexes **1−4** lie at relatively high wavelengths ($\lambda_{max} > 500$ nm) because the donor effect the NCS ligands destabilizes the HOMO.[30] The acceptor (bpy-R)/donor (NCS⁻) combination of ligands ensures absorbance in the middle of the visible region, which is required for the sensitizer function. Upon reduction, this MLCT band gets shifted, and a second IL transition, $\pi^*(7) \rightarrow \pi^*(10)$,[27] of the radical anion (bpy-R)•⁻ emerges at about 600 nm.

During oxidation, e.g., of **3** to the Ru^III form **3⁺** (Scheme 3), UV−vis spectroelectrochemistry reveals a change from the MLCT absorption at 510−550 nm for the neutral species to LMCT bands at lower energy (≈700 nm; Figure 10 and Table 6). This charge has been reported previously for such related compounds.[5e−g] LMCT transitions originating from π(NCS) to
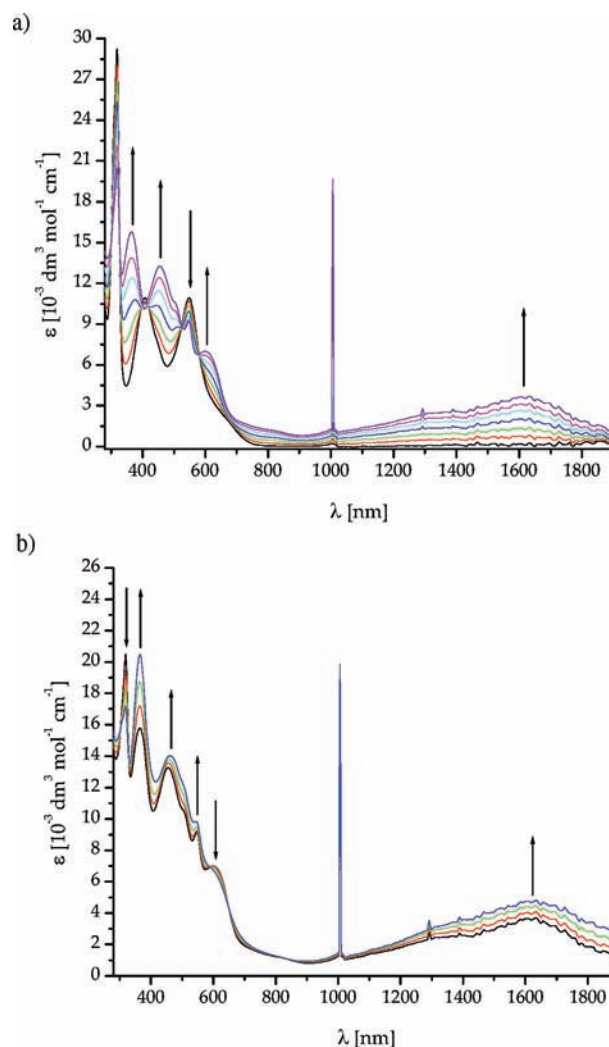
Figure 8. UV−vis spectroelectrochemical response of **2** during the first (a) and second reduction (b) in DMF/0.1 M Bu₄NPF₆.

partially unoccupied metal d orbitals are well established, e.g., forming the basis of the analytical test for Fe^III.[31]

Optimized structural parameters of the parent complex **1** (Table 2) reasonably well describe the experimental data.[5d] In the case of the one-electron-oxidized species **1⁺**, the geometry optimizations were performed for all three possible N-bonded (−NCS) and S-bonded (−SCN) isomers. Figure S2 in the Supporting Information depicts these geometries of isomers and shows the nonlinear Ru−S−C arrangement in the case of the S-bonded ligands. The calculations confirm that the all-(−NCS) isomer is more stable, by about 0.36 eV. In contrast, S coordination of thiocyanate can be expected with less π-accepting coligands and in protic media,[10a] which produce hydrogen bonding to the terminal N atom.

The calculated structural data (Table 2) exhibit a trend for the RuNCS moieties, which is illustrated in terms of charge-dependent bond orders by Scheme 4. The observed low-energy shift of 34−83 cm⁻¹ upon oxidation (Table 3) reflects the decrease in the N−C(S) bond order as a consequence of the overall decreasing bond alternancy (Scheme 4).

■ CONCLUSION

In addition to further evidence supporting the established "MLCT situation" (Scheme 5) of complexes [Ru^II(bpy-

Table 6. Absorption Maxima of Compounds 1−4 Following UV−Vis−NIR

	λ_{max} [nm] (ε [$\times 10^{-3}$ M^{-1} cm^{-1}])			
	1	**2**	**3**	**4**
oxidation	301 (59), 456 (17.2), 582 (sh), 749 (6.4)	a, b	360 (17.3), 450 (sh), 570 (20.9), 694 (16.7)	299 (94), 348 (sh), 521 (18.8), 721 (8.9)
neutral state	300 (58), 363 (30.3), 514 (29.7)	318 (29.2), 408 (10.9), 548 (10.9)	358 (25.0), 524 (18.6)	298 (98), 358 (35), 517 (31.5)
1. reduction	a	319 (20.5), 364 (15.8), 455 (13.3), 599 (7.0, sh), 1350 (sh), 1610 (3.6), ≈3300^c	a	a
2. reduction	b	364 (20.4), 461 (14.0), 544 (9.8, sh), 1350 (sh), 1610 (4.8)	b	b

^{a}Redox form insufficiently stable on the spectroelectrochemical time scale. ^{b}Not measured. ^{c}Broad band (band half-width $\Delta\nu_{1/2} \geq 1500$ cm^{-1}); maximum obscured by vibrational absorption.

a)

b)
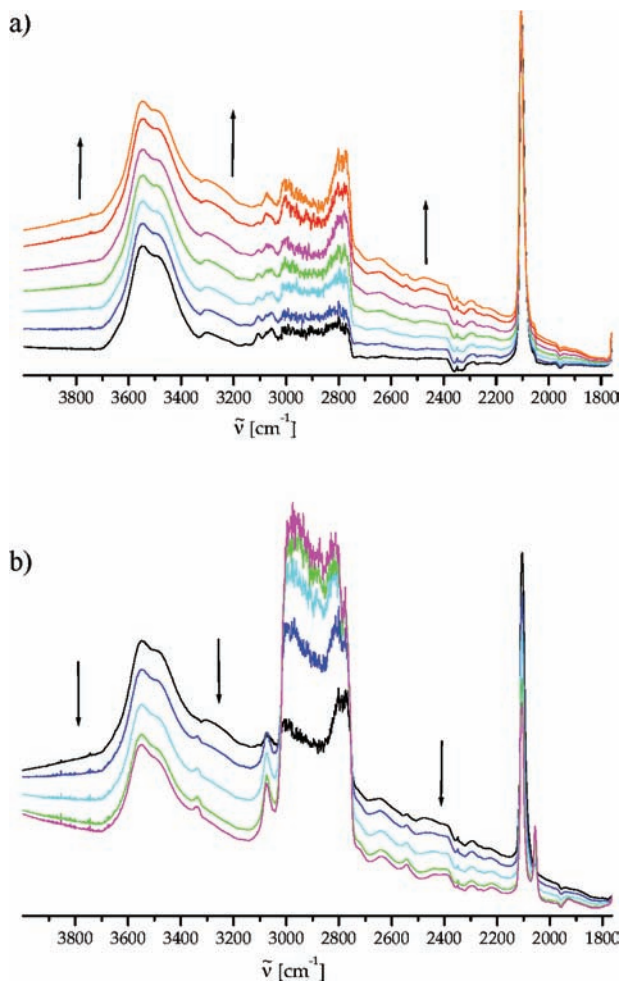
Figure 9. IR spectroelectrochemical response of **2** during the first (a) and second reduction (b) in DMF/0.1 M Bu$_4$NPF$_6$ at high wavenumbers (invariant bands at 3480 (sh) and 3550 cm^{-1} from the solvent).

Scheme 3
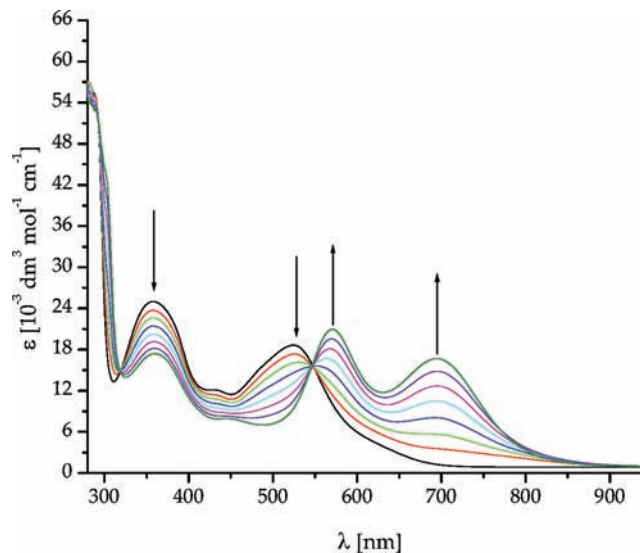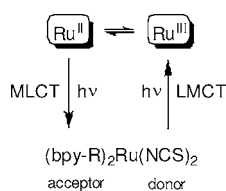
Figure 10. UV−vis spectroelectrochemical response of **3** during oxidation in DMF/0.1 M Bu$_4$NPF$_6$.

Scheme 4

Scheme 5

$\nu_{N-C(S)}$/cm^{-1}		λ_{max}/nm
2071, 2033 (**3$^+$**)	[Ru^{III}(bpy-R)$_2$(NCS)$_2$]$^+$	570, 694 (LMCT; **3$^+$**)
	$-$ e$^-$ ⇅ + e$^-$	
2103 (**2**)	[Ru^{II}(bpy-R)$_2$(NCS)$_2$]	408, 548 (MLCT; **2**)
	$-$ e$^-$ ⇅ + e$^-$	
2105 (**2$^-$**)	[Ru^{II}(bpy-R)(bpy-R$^{\bullet-}$)(NCS)$_2$]$^-$	455 (MLCT), 599 (IL), 1610 (IL), 3300 (LL'IVCT; **2$^-$**)
	$-$ e$^-$ ⇅ + e$^-$	
2107 (**2^{2-}**)	[Ru^{II}(bpy-R$^{\bullet-}$)$_2$(NCS)$_2$]$^{2-}$	544 (IL), 1610 (IL; **2^{2-}**)

R)$_2$(NCS)$_2$], the spectroelectrochemical investigation of the reduced and oxidized states of suitable derivatives provide detailed information on the electronic structure. Stepwise reduction of the bipyridine ligands produces NIR and even mid-IR absorption from IL and LL'IVCT (i.e., interligand) electronic transitions while having little influence on the metal and on the N−C(S) stretching frequency. As a result, there is only minor reductive labilization of the nonchelate ligands, a significant issue for application in DSCs. On the other hand, the oxidation is largely metal-centered, as is evident from low-

2102

dx.doi.org/10.1021/ic201825h | Inorg. Chem. 2012, 51, 2097−2104

energy LMCT transitions ($SCN^- \rightarrow Ru^{III}$), but it also affects the thiocyanate ligands: The C—N(S) stretching bands lose their accidental degeneracy and experience a low-energy shift, reflecting a decrease of the C—N bond order. DFT calculations confirming these trends and the N coordination of ambidentate thiocyanate yield spin densities of 0.117 for each terminal and potentially electrolyte-contacting S atom in [Ru-(bpy)$_2$(NCS)$_2$]$^+$.

■ ASSOCIATED CONTENT

Ⓢ Supporting Information

EPR spectra of **3**$^+$ and **2**$^-$ (Figure S1) and DFT-calculated structures of **1**$^+$ and NCS/SCN linkage isomers (Figure S2). This material is available free of charge via the Internet at http://pubs.acs.org.

■ AUTHOR INFORMATION

Corresponding Author
*E-mail: kaim@iac.uni-stuttgart.de.
Notes
The authors declare no competing financial interest.

■ ACKNOWLEDGMENTS

■ REFERENCES

(1) (a) O'Regan, B.; Grätzel, M. *Nature* **1991**, *353*, 737. (b) Grätzel, M. *Inorg. Chem.* **2005**, *44*, 6841. (c) Grätzel, M. *J. Photochem. Photobiol. C: Photochem. Rev.* **2003**, *4*, 145. (d) Grätzel, M. *Acc. Chem. Res.* **2009**, *42*, 1788. (e) Nazeeruddin, M. K.; Kay, A.; Rodicio, I.; Humphry-Baker, R.; Müller, E.; Liska, P.; Vlachopoulos, N.; Grätzel, M. *J. Am. Chem. Soc.* **1993**, *115*, 6382.

(2) Hamann, T. W.; Jensen, R. A.; Martinson, A. B. F.; Van Ryswyk, H.; Hupp, J. T. *Energy Environ. Sci.* **2008**, *1*, 66.

(3) (a) Nguyen, P. T.; Lam, B. X. T.; Andersen, A. R.; Hansen, P. E.; Lund, T. *Eur. J. Inorg. Chem.* **2011**, 2533. (b) Giribabu, L.; Bessho, T.; Srinivasu, M.; Vijaykumar, C.; Soujanya, Y.; Reddy, V. G.; Reddy, P. Y.; Yum, J.-H.; Grätzel, M.; Nazeeruddin, M. K. *Dalton Trans.* **2011**, *40*, 4497. (c) Chang, W.-C.; Chen, H.-S.; Li, T.-Y.; Hsu, N.-M.; Tingare, Y. S.; Li, C.-Y.; Liu, Y.-C.; Su, C.; Li, W.-R. *Angew. Chem.* **2010**, *122*, 8337; *Angew. Chem., Int. Ed.* **2011**, *49*, 8161. (d) Wang, P.; Klein, C.; Humphry-Baker, R.; Zakeeruddin, S. M.; Grätzel, M. *J. Am. Chem. Soc.* **2005**, *127*, 808. (e) Yang, S.-H.; Wu, K.-L.; Chi, Y.; Cheng, Y.-M.; Chou, P. T. *Angew. Chem.* **2011**, *123*, 8420; *Angew. Chem. Int Ed.* **2011**, *50*, 8270.

(4) (a) Chou, C.-C.; Wu, K.-L.; Chi, Y.; Hu, W.-P.; Yu, S. J.; Lee, G.-H.; Lin, C.-L.; Chou, P.-T. *Angew. Chem.* **2011**, *123*, 2102; *Angew. Chem., Int. Ed.* **2011**, *50*, 2054. (b) Nguyen, P. T.; Degn, R.; Nguyen, H. T.; Lund, T. *Sol. Energy Mater. Sol. Cells* **2009**, *93*, 1939. (c) Cecchet, F.; Gioacchini, A. M.; Marcaccio, M.; Paolucci, F.; Roffia, S.; Alebbi, M.; Bignozzi, C. A. *J. Phys. Chem. B* **2002**, *106*, 3926. (d) Hamann, T. W.; Ondersma, J. W. *Energy Environ. Sci.* **2011**, *4*, 370. (e) Tuikka, M.; Hirva, P.; Rissanen, K.; Korppi-Tommola, J.; Haukka, M. *Chem. Commun.* **2011**, *47*, 4499.

(5) (a) Shklover, V.; Nazeerudddin, M.-K.; Zakeeruddin, S. M.; Barbé, C.; Kay, A.; Haibach, T.; Steurer, W.; Hermann, R.; Nissen, H.-U.; Grätzel, M. *Chem. Mater.* **1997**, *9*, 430. (b) Shklover, V.; Ovchinnikov, Yu. E.; Braginsky, L. S.; Zakeeruddin, S. M.; Grätzel, M. *Chem. Mater.* **1998**, *10*, 2533. (c) Nazeeruddin, Md. K.; Zakeeruddin, S. M.; Humphry-Baker, R.; Jirousek, M.; Liska, P.; Vlachopoulos, N.; Shklover, V.; Fischer, C.-H.; Grätzel, M. *Inorg. Chem.* **1999**, *38*, 6298.

(d) Herber, R. H.; Nan, G.; Potenza, J. A.; Schugar, H. J.; Bino, A. *Inorg. Chem.* **1989**, *28*, 938. (e) Kuang, D.; Iti, S.; Wenger, B.; Klein, C.; Moser, J. E.; Humphry-Baker, R.; Zakeeruddin, S. M.; Grätzel, M. *J. Am. Chem. Soc.* **2006**, *128*, 4146. (f) Li, X.; Nazeeruddin, S.; Thelakkat, M.; Barnes, P. R. F.; Vilar, R.; Durrant, J. R. *Phys. Chem. Chem. Phys.* **2011**, *13*, 1575. (g) Fattori, A.; Peter, L. M.; McCall, K. R.; Robertson, N.; Marken, F. *J. Solid State Electrochem.* **2010**, *14*, 1929. (h) Cecchet, F.; Gioacchini, A. M.; Marcaccio, M.; Paolucci, F.; Roffia, S.; Alebbi, M.; Bignozzi, C. A. *J. Phys. Chem. B* **2002**, *106*, 3926. (i) Braterman, P. S.; Song, J.-I.; Peacock, R. D. *Spectrochim. Acta* **1992**, *48A*, 899.

(6) (a) De Angelis, F.; Fantacci, S.; Selloni, A. *Nanotechnology* **2008**, *19*, 424002. (b) Nazeeruddin, M. K.; De Angelis, F.; Fantacci, S.; Selloni, A.; Viscardi, G.; Liska, P.; Ito, S.; Takeru, B.; Grätzel, M. *J. Am. Chem. Soc.* **2005**, *127*, 16835. (c) Guillemoles, J. F.; Barone, V.; Joubert, L.; Adamo, C. *J. Phys. Chem. A* **2002**, *106*, 11354. (d) Hallett, A. J.; Jones, J. E. *Dalton Trans.* **2011**, *40*, 3871.

(7) Kaim, W.; Fiedler, J. *Chem. Soc. Rev.* **2009**, *38*, 3373.

(8) Pearson, P.; Bond, A. M.; Deacon, G. B.; Forsyth, C.; Spiccia, L. *Inorg. Chim. Acta* **2008**, *361*, 601.

(9) Gütlich, P.; van Koningsbruggen, P. J.; Renz, F. *Struct. Bonding (Berlin)* **2004**, *107*, 27.

(10) (a) Vandenburgh, L.; Buck, M. R.; Freedman, D. A. *Inorg. Chem.* **2008**, *47*, 9134. (b) Nazeeruddin, Md. K.; Grätzel, M. *J. Photochem. Photobiol., A* **2001**, *145*, 79. (c) Kakoti, M.; Chaudhury, S.; Deb, A. K.; Goswami, S. *Polyhedron* **1993**, *12*, 783. (d) Burmeister, J. L. *Coord. Chem. Rev.* **1990**, *106*, 77. (e) Turco, A.; Pecile, C. *Nature* **1961**, *191*, 66. (f) Brewster, T. P.; Ding, W.; Schley, N. D.; Hazari, N.; Batista, V. S.; Crabtree, R. H. *Inorg. Chem.* **2011**, *50*, 11938.

(11) Nazeeruddin, M. K.; Grätzel, M. *Inorg. Synth.* **2002**, 185.

(12) Krejčik, M.; Danek, M.; Hartl, F. *J. Electroanal. Chem. Interfacial Electrochem.* **1991**, *317*, 179.

(13) Kaim, W.; Ernst, S.; Kasack, V. *J. Am. Chem. Soc.* **1990**, *112*, 173.

(14) Frisch, M. J. et al. *Gaussian 09*, revision A.02; Gaussian, Inc.: Wallingford, CT, 2009.

(15) te Velde, G.; Bickelhaupt, F. M.; van Gisbergen, S. J. A.; Fonseca Guerra, C.; Baerends, E. J.; Snijders, J. G.; Ziegler, T. *J. Comput. Chem.* **2001**, *22*, 931.

(16) *ADF 2010.01*; SCM, Vrije Universiteit: Amsterdam, The Netherlands, 2010; http://www.scm.com.

(17) Hariharan, P. H.; Pople, J. A. *Theor. Chim. Acta* **1973**, *28*, 213.

(18) Andrae, D.; Haeussermann, U.; Dolg, M.; Stoll, H.; Preuss, H. *Theor. Chim. Acta* **1990**, *77*, 123.

(19) Perdew, J. P.; Burke, K.; Enzerhof, M. *Phys. Rev. Lett.* **1996**, *77*, 3865.

(20) Adamo, C.; Barone, V. *J. Chem. Phys.* **1999**, *110*, 6158.

(21) Becke, A. D. *J. Chem. Phys.* **1993**, *98*, 5648.

(22) (a) Becke, A. D. *Phys. Rev. A* **1988**, *38*, 3098. (b) Perdew, J. P.; Wang, Y. *Phys. Rev. B* **1992**, *45*, 13244. (c) Perdew, J. P. *Phys. Rev. B* **1986**, *33*, 8822.

(23) (a) van Lenthe, E.; van der Avoird, A.; Wormer, P. E. S. *J. Chem. Phys.* **1998**, *108*, 4783. (b) van Lenthe, E.; van der Avoird, A.; Wormer, P. E. S. *J. Chem. Phys.* **1997**, *107*, 2488.

(24) Cossi, M.; Rega, N.; Scalmani, G.; Barone, V. *J. Comput. Chem.* **2003**, *24*, 669.

(25) Juris, A.; Balzani, V.; Barigelletti, F.; Campagna, S.; Belser, P.; von Zelewsky, A. **1988**, *84*, 85.

(26) (a) Hindson, C. M.; Francis, P. S.; Hanson, G. R.; Barnett, N. W. *Chem. Commun.* **2011**, *47*, 7806. (b) Patra, S.; Sarkar, B.; Mobin, S. M.; Kaim, W.; Lahiri, G. K. *Inorg. Chem.* **2003**, *42*, 6469. (c) Reynolds, P. A.; Cable, J. W.; Sobolev, A. N.; Figgis, B. N. *J. Chem. Soc., Dalton Trans.* **1998**, 559. (d) Jarrett, H. S. *J. Chem. Phys.* **1957**, *27*, 1298.

(27) Braterman, P. S.; Song, J.-I.; Wimmer, F. M.; Wimmer, S.; Kaim, W.; Klein, A.; Peacock, R. D. *Inorg. Chem.* **1992**, *31*, 5084.

(28) (a) Kaim, W.; Reinhardt, R.; Sieger, M. *Inorg. Chem.* **1994**, *33*, 4453. (b) Shida, T. *Electronic Absorption Spectra of Radical Ions*; Elsevier: Amsterdam, The Netheralands, 1988.

(29) (a) Maji, S.; Sarkar, B.; Mobin, S. M.; Fiedler, J.; Kaim, W.; Lahiri, G. K. *Dalton Trans.* **2007**, 2411. (b) Khusniyarov, M. M.; Harms, K.; Burghaus, O.; Sundermeyer, J.; Sarkar, B.; Kaim, W.; van

Slageren, J.; Duboc, C.; Fiedler, J. *Dalton Trans.* **2008**, 1355. (c) Kaim, W. *Coord. Chem. Rev.* **2011**, *255*, 2503.

(30) Ernst, S. D.; Kaim, W. *Inorg. Chem.* **1989**, *28*, 1520.

(31) Mihaljević, B.; Katušin-Ražem, B.; Ražem, D. *Free Radical Biol. Med.* **1996**, *21*, 53.